The Contribution of Ligand Flexibility to Metal Center Geometry Modulated Thermal Cyclization of Conjugated Pyridine and Quinoline Metalloenediynes of Copper(I) and Copper(II)

Diwan S. Rawat,[†] Pedro J. Benites,[†] Christopher D. Incarvito,[‡] Arnold L. Rheingold,[‡] and Jeffrey M. Zaleski*,[†]

[†]Department of Chemistry, Indiana University, Bloomington, Indiana 47405, and [‡]Department of Chemistry and Biochemistry, University of Delaware, Newark, Delaware 19716

Received January 3, 2001

We report the syntheses, reactivities, and structure evaluations of a series of Cu(I) and Cu(II) metalloenediynes of conjugated 1,6-bis(pyridine-3)hex-3-ene-1,5-diyne (PyED, **7**) and 1,6-bis(quinoline-3)hex-3-ene-1,5-diyne (QnED, **8**) enediyne ligands, as well as their benzoenediyne analogues. Differential scanning calorimetry demonstrates that the $[Cu(PyED)_2](NO_3)_2$ (**11**) exhibits a Bergman cyclization temperature (156 °C) which is dramatically reduced from that of the corresponding $[Cu(PyED)_2](PF_6)$ (**19**) analogue (326 °C), indicating that large differences in the reactivities of these metalloenediynes can be accessed by variations in metal oxidation state. The distorted, 4-coordinate dichloride compound $Cu(PyED)(Cl)_2$ (**15**) exhibits a cyclization temperature (265 °C) between those of **11** and **19**, suggesting that variation in geometry of the copper center is responsible for the wide range of reactivities. Similar results are obtained for the benzoenediyne and quinoline analogues. The structures of the Cu(II) systems have also been evaluated by a combination of electronic absorption and EPR spectroscopies which reveal tetragonal, 6-coordinate structures for the bis(enediyne) complexes, and tetrahedrally distorted 4-coordinate Cu(enediyne)Cl_2 species. For the bis(quinoline) enediyne derivatives **12** and **14** the larger *g*-anisotropy ($g_{\|} = 2.27-2.28$; $g_{\perp} = 2.06-2.07$) indicates strong oxygen coordination from counterion. Molecular mechanics/dynamics calculations reveal that the geometries of these metal centers force the alkyne termini to a wide range of distances (3.85−4.20 Å), thereby accounting for the variability in Bergman cyclization temperatures. Overall, the results show that ligand rigidity plays a prominent role in the conformational response of the enediyne to metal center geometry, which results in enhanced variations in the Bergman cyclization temperatures between complexes of different geometries.

Introduction

The enediyne antibiotics are intriguing chemical structures that form 1,4-phenyl diradical intermediates capable of cleaving DNA by H-atom abstraction.[1−14] A plethora of synthetic and theoretical studies of these molecules has rendered considerable information regarding the key geometric and electronic structural requirements needed to induce Bergman cyclization at experimentally accessible temperatures.[15−38] One of the key structural

* Author to whom correspondence should be addressed (E-mail: zaleski@indiana.edu).
[†] Indiana University.
[‡] University of Delaware.

(1) Smith, A. L.; Nicolaou, K. C. *J. Med. Chem.* **1996**, *39*, 2103−2117.
(2) Paloma, L. G.; Smith, J. A.; Chazin, W. J.; Nicolaou, K. C. *J. Am. Chem. Soc.* **1994**, *116*, 3697−3708.
(3) Kappen, L. S.; Goldberg, I. H. *Biochemistry* **1983**, *22*, 4872−4878.
(4) Zein, N.; McGahren, W. J.; Morton, G. O.; Ashcroft, J.; Ellestead, G. A. *J. Am. Chem. Soc.* **1989**, *111*, 6888−6890.
(5) De Voss, J. J.; Townsend, C. A.; Ding, W.-D.; Morton, G. O.; Ellestad, G. A.; Zein, N.; Tabor, A. B.; Schreiber, S. L. *J. Am. Chem. Soc.* **1990**, *112*, 9669−9670.
(6) Hangeland, J. J.; DeVoss, J. J.; Heath, J. A.; Townsend, C. A.; Ding, W.-D.; Ashcroft, J. S.; Ellestad, G. A. *J. Am. Chem. Soc.* **1992**, *114*, 9200−9202.
(7) Dedon, P.; Salzberg, A. A.; Xu, J. *Biochemistry* **1993**, *32*, 3617−3622.
(8) Christner, D. F.; Frank, B. L.; Kozarich, J. W.; Stubbe, J.; Golik, J.; Doyle, T. W.; Rosenberg, I. E.; Krishnan, B. *J. Am. Chem. Soc.* **1992**, *114*, 8763−8767.
(9) Sugiura, Y.; Suzuki, T.; Kuwahara, J.; Tanaka, H. *Biochem. Biophys. Res. Commun.* **1982**, *105*, 1511−1518.
(10) Sugiura, Y.; Shiraki, T.; Konishi, M.; Oki, T. *Proc. Natl. Acad. Sci. U.S.A.* **1990**, *87*, 3831−3835.
(11) Shiraki, T.; Sugiura, Y. *Biochemistry* **1990**, *29*, 9795−9798.
(12) Shiraki, T.; Uesugi, M.; Sugiura, Y. *Biochem. Biophys. Res. Commun.* **1992**, *188*, 584−589.
(13) Xu, Y.; Zhen, Y.; Goldberg, I. H. *Biochemistry* **1994**, *33*, 5947−5954.
(14) Matsumoto, T.; Okuno, Y.; Sugiura, Y. *Biochem. Biophys. Res. Commun.* **1993**, *195*, 659−666.
(15) Takahashi, T.; Tanaka, H.; Yamada, H.; Matsumoto, T.; Sugiura, Y. *Angew. Chem., Int. Ed. Engl.* **1996**, *35*, 1835.
(16) Nicolaou, K. C.; Zuccarello, G.; Riemer, C.; Estevez, V. A.; Dai, W.-M. *J. Am. Chem. Soc.* **1992**, *114*, 7360−7371.
(17) Nicolaou, K. C.; Dai, W.-M.; Wendeborn, S. V.; Smith, A. L.; Torisawa, Y.; Maligres, P.; Hwang, C.-K. *Angew. Chem., Int. Ed. Engl.* **1991**, *30*, 1032−1036.
(18) Nicolaou, K. C.; Liu, A.; Zeng, Z.; McComb, S. *J. Am. Chem. Soc.* **1992**, *114*, 9279.
(19) Nicolaou, K. C.; Smith, A. L.; Wendeborn, S. V.; Hwang, C.-K. *J. Am. Chem. Soc.* **1991**, *113*, 3106−3114.
(20) Nicolaou, K. C.; Tsay, S.-C.; Suzuki, T.; Joyce, G. F. *J. Am. Chem. Soc.* **1992**, *114*, 7555−7557.
(21) Nicolaou, K. C.; Smith, A. L. *Acc. Chem. Res.* **1992**, *25*, 497−503.
(22) Nicolaou, K. C.; Dai, W.-M.; Tsay, S.-C.; Estevez, V. A.; Wrasidlo, W. *Science* **1992**, *256*, 1172−1178.
(23) Nicolaou, K. C.; Dai, W.-M. *Angew. Chem., Int. Ed. Engl.* **1991**, *30*, 1387−1416.
(24) Nicolaou, K. C.; Smith, B. M.; Ajito, K.; Komatsu, H.; Gomez-Paloma, L.; Tor, Y. *J. Am. Chem. Soc.* **1996**, *118*, 2303−2306.
(25) Nicolaou, K. C.; Li, T.; Nakada, M.; Hummel, C. W.; Hiatt, A.; Wrasidlo, W. *Angew. Chem., Int. Ed. Engl.* **1994**, *33*, 183−186.
(26) Aiyar, J.; Danishefsky, S. J.; Crothers, D. M. *J. Am. Chem. Soc.* **1992**, *114*, 7552.
(27) Aiyar, J.; Hitchcock, S. A.; Denhart, D.; Liu, K. K. C.; Danishefsky, S. J.; Crothers, D. M. *Angew. Chem., Int. Ed. Engl.* **1994**, *33*, 855−856.
(28) Zein, N.; Sinha, A. M.; McGahren, W. J.; Ellestad, G. A. *Science* **1988**, *240*, 1198−1201.

10.1021/ic010014l CCC: $20.00
Published on Web 03/08/2001

parameters is the distance between alkyne termini[23,39] and its convoluted relationship with the corresponding ring strain for monocyclic enediynes.[40−43] Both of these features influence the activation barrier to enediyne cyclization, but their independent contributions are difficult to quantitate.[44] This notwithstanding, it is clear that the geometric constraints imposed by the ring-closing motif at the 1,6-positions of the enediyne strongly affect the thermal cyclization temperatures of the enediynes.

More recently, metal-chelating enediyne ligands have been synthesized in order to investigate the role transition metals may play in controlling and modulating Bergman cyclization temperatures,[45−51] with the goal of achieving stable compounds that can be triggered to react under physiological conditions. Since the structures of acyclic enediynes are not sterically restricted, many of them exhibit high thermal cyclization temperatures in the pure liquid and/or solid states. However, upon chelation to transition metals that promote formation of planar metallocycle geometries (e.g., Cu(II), Pd(II), Pt(II)), the Bergman cyclization temperatures are dramatically reduced.[45,47,49−51] In contrast, for transition metals that have ligand field preferences for tetrahedral geometries (e.g., Cu(I), Pd(0), Hg(II)), either cyclization temperatures are only modestly decreased from the free ligand values or the cyclization reactions are completely inhibited.[45,48,49] The increase in cyclization temperature for the tetrahedral vs planar metalloenediyne ring results from the high activation energy required to bring the alkyne termini into close proximity in the transition state from the tetrahedral ground state structure.[45,48,49]

A more subtle issue than the immediate geometry of the metallocycle is the rigidity of the enediyne ligand itself. Reports to date on metal-assisted Bergman cyclization of enediynes have not examined how the rigidity of the ligand may affect the magnitude of the variation in the cyclization temperature upon chelation to a given transition metal. From first principles, the more conformationally flexible the enediyne chelate, as defined by the greater number of sp^3 atoms between the alkyne carbons and metal-binding functionality, the lower the cyclization temperature should be. In this case, the net effect upon chelation should be a significant but somewhat damped influence of the metal on the Bergman cyclization temperature of the resulting complex due to the inherent flexibility of the organic framework. Thus, the greatest modulation of the Bergman cyclization temperature due to metal coordination should result from rigid metalloenediyne structures possessing metal-binding functional groups fused directly to the 1,6-alkyne termini.

To this end, we report the syntheses, structural evaluations, and thermal reactivities of a series of Cu(I) and Cu(II) metalloenediynes featuring rigid enediyne ligand frameworks with bis(pyridine) and bis(quinoline) metal-chelating functionalities. These complexes conform to the principle that the geometry of the metal center modulates the enediyne activation barrier by exhibiting control of the Bergman cyclization temperatures based on metal oxidation state.[48,49] Moreover, the inherent inflexibility of the ligand framework is reflected in the increased magnitude of the responsiveness of the ligand to changes in metal center geometry over more flexible Cu(I) and Cu(II) metalloenediyne analogues previously reported.[49]

Experimental Section

Materials. All air-sensitive reactions were carried out under inert atmosphere (nitrogen) using Schlenk and drybox techniques. Hydrocarbon solvents such as ether and benzene were dried by distillation over sodium/benzophenone. Dichloromethane and n-butylamine were dried and distilled from calcium hydride. NMR solvents were dried and degassed before use.

Chemicals. All chemicals used in the syntheses were of the highest purity available from Aldrich and Fluka and used as received. The organic enediyne compounds were purified by flash chromatography using HPLC grade solvents.

Physical Measurements. Electron paramagnetic resonance spectra were recorded on an ESP 300 Bruker instrument under the following conditions: microwave frequency, ~9.5 GHz; microwave power, >10 mW; modulation amplitude, 2−5 G; modulation frequency; 100 kHz; receiver gain, $2.5-5 \times 10^4$. Powder samples for EPR were prepared by cogrinding the Cu(II) complexes (0.01 wt %) with KBr. Cocrystallization of the Cu(II) samples with a guest matrix (for elucidation of $A_{||}$) was not performed due to the potential formation of centers with varying ligand:copper stoichiometries. ^{1}H and ^{13}C NMR were recorded on a VXR 400 NMR spectrometer, using the residual proton resonance of the solvent as an internal reference. The multiplicity of the ^{13}C signals was determined by the DEPT technique. High-resolution EI mass spectra were acquired on a Kratos MS-80 mass spectrometer that was interfaced with a Kratos DS 90 data system. ESI and FAB MS data were obtained at University of Illinios with a Micromass Quattro I mass spectrometer. Electronic absorption spectra in the solid state (Nujol) were obtained on a Perkin-Elmer Lambda 19 UV/vis/near-IR spectrometer. For the ligand field UV−vis measurements, the experimental error in the measured energies is $= 5$ cm^{-1} at 13 500 cm^{-1}. Infrared (KBr pellet) spectra were recorded on a Nicolet 510P FT IR spectrometer. Elemental analyses on the samples were obtained from Atlantic Microlab, INC. Differential scanning calorimetry (DSC) traces were recorded on a General V4.1 DuPont 910 DSC differential scanning calorimeter coupled to DuPont Thermal Analyst 2100 at a heating rate of 10 °C min^{-1}.

(29) Drak, J.; Iwasawa, N.; Danishefsky, S. J.; Crothers, D. M. *Proc. Natl. Acad. Sci. U.S.A.* **1991**, *88*, 7464−7468.
(30) Depew, K. M.; Zeman, S. M.; Boyer, S. H.; Denhart, D. J.; Ikemoto, N.; Danishefsky, S. J.; Crothers, D. M. *Angew. Chem., Int. Ed. Engl.* **1996**, *35*, 2797−2801.
(31) Li, H.; Zeng, Z.; Estevez, V. A.; Baldenius, K. U.; Nicolaou, K. C.; Joyce, G. F. *J. Am. Chem. Soc.* **1994**, *116*, 3709−3715.
(32) Liu, C.; Smith, B. M.; Ajito, K.; Komatsu, H.; Gomez-Paloma, L.; Li, T.; Theodorakis, E. A.; Nicolaou, K. C.; Vogt, P. K. *Proc. Natl. Acad. Sci. U.S.A.* **1996**, *93*, 940−944.
(33) Ho, S. N.; Boyer, S. H.; Schreiber, S. L.; Danishefsky, S. J.; Crabtree, R. G. *Proc. Natl. Acad. Sci. U.S.A.* **1994**, *91*, 9203−9207.
(34) Elbaum, D.; Porco, J. A., Jr.; Stout, T. J.; Clardy, J.; Schreiber, S. L. *J. Am. Chem. Soc.* **1995**, *117*, 211−225.
(35) Myers, A. G.; Fraley, M. E.; Tom, N. J.; Cohen, S. B.; Madar, D. J. *Chem. Biol.* **1995**, *2*, 33−43.
(36) Myers, A. G.; Cohen, S. B.; Tom, N. J.; Madar, D. J.; Fraley, M. E. *J. Am. Chem. Soc.* **1995**, *117*, 7574−7575.
(37) Shair, M. D.; Yoon, T.; Chou, T. C.; Danishefsky, S. J. *Angew. Chem., Int. Ed. Engl.* **1994**, *33*, 2477−2479.
(38) Chatterjee, M.; Mah, S. C.; Tullius, T. D.; Townsend, C. A. *J. Am. Chem. Soc.* **1995**, *117*, 8074−8082.
(39) Nicolaou, K. C.; Smith, A. L.; Yue, E. W. *Proc. Natl. Acad. Sci., U.S.A.* **1993**, *90*, 5881−5888.
(40) Magnus, P.; Lewis, R. T.; Huffman, J. C. *J. Am. Chem. Soc.* **1988**, *110*, 6921−6923.
(41) Magnus, P.; Fortt, S.; Pitterna, T.; Snyder, J. P. *J. Am. Chem. Soc.* **1990**, *112*, 4986−4987.
(42) Snyder, J. P. *J. Am. Chem. Soc.* **1989**, *111*, 7630−7632.
(43) Snyder, J. P. *J. Am. Chem. Soc.* **1990**, *112*, 5367−5369.
(44) Schreiner, P. R. *J. Am. Chem. Soc.* **1998**, *120*, 4184−4190.
(45) Warner, B. P.; Millar, S. P.; Broene, R. D.; Buchwald, S. L. *Science* **1995**, *269*, 814−816.
(46) (a) Konig, B. *Eur. J. Org. Chem.* **2000**, 381−385. (b) O'Connor, J. M.; Lee, L. I.; Gantzel, P.; Rheingold, A. L.; Lam, K.-C. *J. Am. Chem. Soc.* **2000**, *122*, 12057−12058.
(47) Konig, B.; Pitsch, W.; Thondorf, I. *J. Org. Chem.* **1996**, *61*, 4258−4261.
(48) (a) Coalter, N.; Concolino, T. E.; Streib, W. E.; Hughes, C. G.; Rheingold, A. L.; Zaleski, J. M. *J. Am. Chem. Soc.* **2000**, *122*, 3112−3117. (b) Schmitt, E. W.; Huffman, J. C.; Zaleski, J. M. *Chem. Commun.* **2001**, 167−168.
(49) Benites, P. B.; Rawat, D. S.; Zaleski, J. M. *J. Am. Chem. Soc.* **2000**, *122*, 7208−7217.
(50) Basak, A.; Shain, J. *Tetrahedron Lett.* **1998**, *39*, 1623−1624.
(51) (a) Basak, A.; Shain, J. C.; Khamrai, T. K.; Rudra, K. R.; Basak, A. *J. Chem. Soc., Perkin Trans. 1* **2000**, 1955−1964. (b) Basak, A.; Rudra, K. R. *Tetrahedron Lett.* **2000**, *41*, 7231−7234.

Crystallographic Structure Determination of 8. A suitable crystal for data collection was selected and mounted with epoxy cement on the tip of a fine glass fiber. Data were collected with a Siemens P4 diffractometer equipped with a SMART/CCD detector.

The systematic absences in the diffraction data are consistent with the reported space group, which yielded chemically reasonable and computationally stable results of refinement. The structure was solved using direct methods and completed by subsequent difference Fourier syntheses and refined by full-matrix least-squares procedures. The molecule lies on a crystallographic mirror plane. The molecule cocrystallized with one molecule of acetonitrile which also lies on a crystallographic mirror plane. The hydrogen atoms of the lattice solvent were located from the electron difference map and allowed to refine. All non-hydrogen atoms were refined with anisotropic displacement coefficients, and the hydrogen atoms, with the exception of those noted, were treated as idealized contributions. All software and sources of the scattering factors are contained in the SHELXTL (5.1) program library (G. Sheldrick, Siemens XRD, Madison, WI).

Molecular Modeling. Molecular mechanics calculations at the MMX force field level were performed using PCModel v.7.0 (Serena Software) on a Silicon Graphics O2R5000 Unix workstation.

Synthesis of 3-Trimethylsilylethynylpyridine[52] (3). To a mixture of 3-bromopyridine (8.0 g, 0.05 mol) and $(Ph_3P)_4Pd$ (0.51 g, 10 mol %) in diisopropylamine (80.0 mL) was added trimethylsilylacetylene (5.95 g, 0.06 mol), and the solution was stirred at 85 °C for 8.0 h. The reaction mixture was subsequently filtered to remove the resulting salt formed during the reaction. The solvent was then removed by distillation. The crude compound was chromatographed on silica gel (5% hexanes/dichloromethane). Yield: 7.5 g (84.7%); viscous oil. R_f: 0.2. ^{1}H NMR ($CDCl_3$): 0.28 (s, 9H), 7.24 (m, 1H), 7.76 (m, 1H), 8.54 (d, J = 5.2 Hz, 1H), 8.70 (s, 1H). ^{13}C NMR ($CDCl_3$): 0.45 (CH_3), 96.97 (C_{quart}), 100.2 (C_{quart}), 119.08 (C_{quart}), 121.56 (CH), 137.49 (CH), 147.44 (CH), 151.42 (CH). MS: m/z 175 (M^+), 160 ($M^+ - CH_3$).

Synthesis of 3-Trimethylsilylethynylquinoline[52] (4). Yield: 90.0%; viscous oil. ^{1}H NMR ($CDCl_3$): 0.28 (s, 9H), 7.48 (t, J = 7.2 Hz, 1H), 7.67 (m, 2H), 8.04 (d, J = 8.4 Hz, 1H), 8.19 (s, 1H), 8.89 (s, 1H). ^{13}C NMR ($CDCl_3$): 0.21 (CH_3), 98.52 (C_{quart}), 102.46 (C_{quart}), 117.62 (C_{quart}), 127.38 (C_{quart}), 127.54 (CH), 127.88 (CH), 129.72 (CH), 130.42 (CH), 139.14 (CH), 147.19 (C_{quart}), 152.59 (CH). MS: m/z 225 (M^+), 210.

Synthesis of 3-Ethynylpyridine[52] (5). A mixture of 3-trimethylsilylethynylpyridine (4.0 g, 0.02 mol), K_2CO_3 (10.0 g, 0.07 mol), and MeOH (200.0 mL) was stirred at room temperature for 1 h. The solvent was removed by distillation after filtration and the product extracted with dichloromethane. The crude product was purified by flash chromatography (dichloromethane). Yield: 1.29 g (55.0%). ^{1}H NMR ($CDCl_3$): 3.22 (s, 1H), 7.25 (m, 1H), 7.76 (d, J = 8.0 Hz, 1H), 8.56 (d, J = 4.4 Hz, 1H), 8.73 (s, 1H). ^{13}C NMR ($CDCl_3$): 80.04 (C_{quart}), 80.85 (CH), 119.88 (C_{quart}), 123.19 (CH), 139.28 (CH), 149.38 (CH), 153.04 (CH). MS: m/z 103 (M^+).

Synthesis of 3-Ethynylquinoline[52] (6). Yield: 65.0%. ^{1}H NMR ($CDCl_3$): 3.27 (s, 1H), 7.55 (t, J = 7.2 Hz, 1H), 7.70−7.78 (m, 2H), 8.09 (d, J = 8.4 Hz, 1H), 8.26 (s, 1H), 8.93 (s, 1H). ^{13}C NMR ($CDCl_3$): 80.75 (CH), 81.18 (C_{quart}), 116.47 (C_{quart}), 127.25 (C_{quart}), 127.60 (CH), 127.84 (CH), 129.68 (CH), 130.61 (CH), 139.56 (CH), 147.35 (C_{quart}), 152.49 (CH). MS: m/z 153 (M^+).

Synthesis of 1,6-Bis(pyridine-3)hex-3-ene-1,5-diyne (PyED, 7). To a mixture of *cis*-1,2-dichloroethylene (0.25 g, 2.58 mmol), *n*-butylamine (0.59 g, 8.1 mmol), $Pd(PPh_3)_4$ (0.17 g, 0.15 mmol), and CuI (0.06 g, 0.30 mmol) in 25 mL of benzene was added 3-ethynylpyridine (0.58 g, 5.7 mmol) in 10.0 mL of benzene at 45 °C over 30 min. The reaction mixture was stirred for 30 min at this temperature. The progress of the reaction was monitored by TLC and ^{1}H NMR. After completion, the solvent was removed and the crude product purified by flash chromatography (ether). Yield: 0.33 g (58.9%). Mp: 86 °C. ^{1}H NMR ($CDCl_3$): 6.23 (s, 2H), 7.34 (m, 2H), 7.82 (d, J = 8.0 Hz, 2H), 8.64 (s, 2H), 8.81 (s, 2H). ^{13}C NMR ($CDCl_3$): 90.0 (C_{quart}), 94.2 (C_{quart}), 120.08 (CH), 120.10 (C_{quart}), 123.43 (CH), 138.68 (CH), 149.26 (CH), 152.47 (CH). IR (KBr, cm^{-1}): 3031, 2931, 2180, 1691, 1554, 1470, 1405, 1019, 815, 800, 961, 699. MS: m/z 230 (M^+).

Synthesis of 1,6-Bis(quinoline-3)hex-3-ene-1,5-diyne (QnED, 8). Yield: 65.0%. Mp: 126 °C. ^{1}H NMR ($CDCl_3$): 6.24 (s, 2H), 7.56 (t, J = 7.2 Hz, 2H), 7.74−7.79 (m, 4H), 8.10 (d, J = 8.4 Hz, 2H), 8.24 (s, 2H), 8.99 (s, 2H). ^{13}C NMR ($CDCl_3$): 90.44 (C_{quart}), 95.52 (C_{quart}), 117.30 (C_{quart}), 120.14 (CH), 127.41 (C_{quart}), 127.67 (CH), 127.99 (CH), 129.69 (CH), 130.65 (CH), 138.72 (CH), 147.29 (C_{quart}), 152.16 (CH). IR (KBr, cm^{-1}): 3060, 2998, 2926, 2182, 1615, 1564, 1487, 1464, 1345, 1284, 999, 954, 901, 855, 780, 748, 648. MS: m/z 330 (M^+).

Synthesis of 1,2-Bis(3-ethynylpyridine)benzene (PybED, 9). To a mixture of 1,2-diiodobenzene (2.0 g, 6.0 mmol), diisopropylamine (3.8 g, 37.6 mmol), $Pd(PPh_3)_2Cl_2$ (0.47 g, 0.35 mmol), and CuI (0.14 g, 0.71 mmol) in 20.0 mL of benzene was added 3-ethynylpyridine (1.4 g, 13.0 mmol) at 45 °C over 30 min. The reaction mixture was stirred for 30 min and the solvent removed under vacuum. The crude product was purified by flash chromatography (dichloromethane/hexanes). Yield: 3.58 g (62.0%). Mp: 53 °C. ^{1}H NMR ($CDCl_3$): 7.27−7.37 (m, 4H), 7.56 (m, 2H), 7.83 (s, 2H), 8.55 (s, 2H), 8.78 (s, 2H). ^{13}C NMR ($CDCl_3$): 90.0 (C_{quart}), 90.8 (C_{quart}), 120.0 (C_{quart}), 123.42 (CH), 124.85 (C_{quart}), 128.88 (CH), 132.28 (CH), 138.64 (CH), 149.05 (CH), 152.37 (CH). IR (KBr, cm^{-1}): 3080, 3061, 2217, 1559, 1486, 1475, 1404, 1021, 809, 798, 765, 700, 626. MS: m/z 280 (M^+).

Synthesis of 1,2-Bis(3-ethynylquinoline)benzene (QnbED, 10). Yield: 60.0%. Mp: 142 °C. ^{1}H NMR ($CDCl_3$): 7.25 (brs, 2H), 7.41 (brs, 2H), 7.67−7.75 (m, 6H), 8.11 (brs, 2H), 8.35 (s, 2H), 9.05 (s, 2H). ^{13}C NMR ($CDCl_3$): 91.4 (C_{quart}), 91.9 (C_{quart}), 116.8 (C_{quart}), 127.3 (C_{quart}), 127.67 (CH), 127.95 (CH), 128.93 (CH), 129.72 (CH), 130.55 (CH), 132.39 (CH), 138.67 (CH), 147.2 (C_{quart}), 152.19 (CH). IR (KBr, cm^{-1}): 3055, 3030, 2209, 1486, 1443, 1015, 900, 783, 756, 747, 664. MS: m/z 380 (M^+).

Synthesis of $[Cu(PyED)_2](NO_3)_2$ (11). A 50 mL round-bottom flask was charged with **7** (0.52 g, 2.3 mmol) dissolved in 15.0 mL of methanol (45 °C). To this mixture, a solution of $Cu(NO_3)_2 \cdot 2.5H_2O$ (0.26 g, 1.0 mmol) in 5.0 mL methanol was slowly added at the same temperature. The reaction mixture was stirred for 16 h. The product was filtered and washed with methanol and dried overnight under vacuum. Yield: 0.64 g (88.4%). Mp: 150−153 °C (dec). IR (KBr, cm^{-1}): 3073, 3020, 2190, 1576, 1479, 1384, 1310, 1196, 813, 748, 696, 657. MS (FAB): 648, 650 ($M^+ + H$) ^{63,65}Cu (M^+ calcd for $C_{32}H_{20}N_4Cu.2NO_3$: 647, 649), 523 ($M^+ - 2NO_3$), 418, 231. Anal. Calcd for $C_{32}H_{20}N_6O_6Cu \cdot 2.5H_2O$: C, 55.45; H, 3.63; N, 12.12. Found: C, 55.45; H, 3.58; N, 11.79.

Synthesis of $[Cu(QnED)_2](NO_3)_2$ (12). Yield: 82.5%. Mp: 167−172 °C (dec). IR (KBr, cm^{-1}): 3038, 2915, 2183, 1479, 1384, 1277, 1011, 910, 805, 783, 758, 693, 634. MS (FAB): 848, 850 ($M^+ + H$), ^{63,65}Cu (M^+ calcd for $C_{48}H_{28}N_4Cu \cdot 2NO_3$: 847, 849), 786 ($M^+ - NO_3$), 723 ($M^+ - 2NO_3$), 518, 331. Anal. Calcd for $C_{48}H_{28}N_6O_6Cu \cdot 2.5H_2O$: C, 64.53; H, 3.69; N, 9.41. Found: C, 64.27; H, 3.46; N, 9.63.

Synthesis of $[Cu(PybED)_2](NO_3)_2$ (13). Yield: 80.0%. Mp: 203−207 °C (dec). IR (KBr, cm^{-1}): 3071, 2942, 2854, 2229, 1488, 1384, 1295, 1194, 1106, 1055, 868, 763, 697. MS (FAB): 748, 750 ($M^+ + H$), ^{63,65}Cu (M^+ Calcd for $C_{40}H_{24}N_4Cu \cdot 2NO_3$: 747, 749), 623 ($M^+ - 2NO_3$), 468, 343, 281. Anal. Calcd for $C_{40}H_{24}N_6O_6 \cdot 2.5H_2O$: C, 60.57; H, 3.68; N, 10.59. Found: C, 60.32,; H, 3.68; N, 10.78.

Synthesis of $[Cu(QnbED)_2](NO_3)_2$ (14). Yield: 80.0%. Mp: 230−234 °C (dec); IR (KBr, cm^{-1}): 3060, 2203, 1490, 1477, 1445, 1384, 1279, 999, 990, 780, 752, 634. MS (FAB): 948, 950 ($M^+ + H$), ^{63,65}Cu (M^+ calcd for $C_{56}H_{32}N_4Cu \cdot 2NO_3$; 947, 949), 823 ($M^+ - 2NO_3$), 568, 443, 381. Anal. Calcd for $C_{56}H_{32}N_4Cu \cdot 2NO_3$: C, 70.92; H, 3.40; N, 8.86. Found: C, 71.2; H, 3.49; N, 9.05.

Synthesis of $Cu(PyED)Cl_2$ (15). In a 50.0 mL round-bottom flask **7** (0.39 g, 1.7 mmol) was dissolved in 10.0 mL methanol at 45 °C. To this solution was added $CuCl_2 \cdot 2H_2O$ (0.29 g, 1.7 mmol) in 5.0 mL of methanol, and the reaction mixture was stirred for 16 h. The solid product was filtered, washed with methanol, and dried under vacuum overnight. Yield: 0.46 g (73.5%). Mp: 260−264 °C (dec). IR (KBr, cm^{-1}): 3074, 2186, 1596, 1481, 1417, 1191, 1059, 919, 807, 745, 688, 656. MS (FAB): 329, 331 ^{63,65}Cu ($M^+ - Cl$), 231. Anal. Calcd for $C_{16}H_{10}N_2Cl_2Cu$: C, 54.67; H, 2.76; N, 7.71. Found: C, 54.41; H, 2.86; N, 7.43.

Synthesis of $Cu(QnED)Cl_2$ (16). Yield: 72.0%. Mp: 230−234 °C (dec). IR (KBr, cm^{-1}): 3043, 2178, 1580, 1498, 1464, 1403, 1146, 959, 915, 777, 746, 634. MS (FAB): 439, 441, ^{63,65}Cu ($M^+ - Cl$),

Scheme 1. Synthesis of Heterocycle-Substituted Alkynes via 3-Bromopyridine and 3-Bromoquinoline Precursors

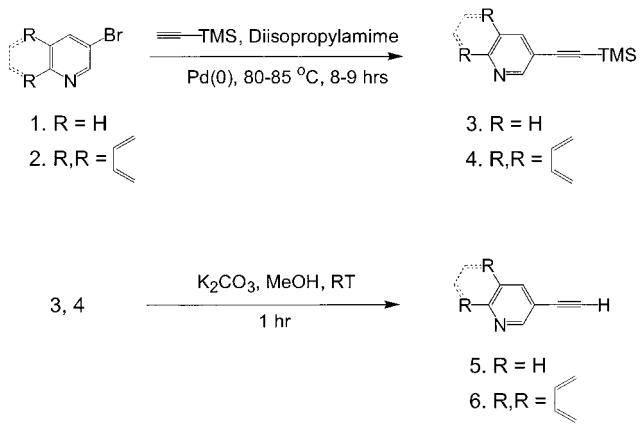

331. Anal. Calcd for $C_{24}H_{14}N_2Cl_2Cu$: C, 62.06; H, 3.02; N, 6.03. Found: C, 62.26; H, 3.30; N, 5.90.

Synthesis of Cu(PybED)Cl$_2$ (17). Yield: 65.0%. Mp: 272−275 °C (dec). IR (KBr, cm^{-1}): 3098, 3061, 3030, 2224, 1598, 1491, 1418, 1192, 1124, 1051, 919, 802, 755, 698, 658. MS (FAB): 378, 380, ^{63,65}Cu (M^+ − Cl), 281. Anal. Calcd for $C_{20}H_{12}Cl_2N_2Cu$: C, 57.89; H, 2.92; N, 6.78. Found: C, 57.99; H, 3.10; N, 6.58.

Synthesis of Cu(QnbED)Cl$_2$ (18). Yield: 67.0%. Mp: 230−234 °C (dec). IR (KBr, cm^{-1}): 3056, 2213, 1617, 1467, 1486, 1460, 1353, 1145, 993, 956, 913, 777, 746. MS (FAB): 479, 481 ^{63,65}Cu (M^+ − Cl), 443, 445 (M^+ − 2Cl), 381. Anal. Calcd for $C_{28}H_{16}Cl_2N_2Cu$: C, 65.50; H, 3.12; N, 5.46. Found: C, 66.35; H, 3.42; N, 5.51.

Synthesis of [Cu(PyED)$_2$]PF$_6$ (19). In a 50 mL Schlenk flask, PyED (**7**) (0.3 g, 1.3 mmol) was dissolved in 15.0 mL of degassed MeOH. To this mixture was slowly added a solution of $[(CH_3CN)_4Cu]PF_6$ (0.24 g, 0.65 mmol) in 10.0 mL of degassed MeOH. The reaction mixture was stirred for 12 h at ambient temperature. The solid product was filtered off, washed with MeOH, and dried under vacuum. Yield: 0.32 g (56.0%). ^{1}H NMR (DMSO-d_6): 6.46 (s, 4H), 7.61 (s, 4H), 8.05 (s, 4H), 8.82 (brs, 8H). ^{13}C NMR (DMSO-d_6): 91.58 (C_{quart}), 94.58 (C_{quart}), 118.85 (C_{quart}), 121.27 (CH), 126.33 (CH), 140.46 (CH), 150.43 (CH), 152.54 (CH). IR (KBr, cm^{-1}): 3064, 2947, 2194, 1568, 1480, 1412, 1173, 1037, 839, 745, 695, 557. MS (FAB): 523, 525 ^{63,65}Cu (M^+ calcd for $C_{32}H_{20}N_4Cu$: 523, 525), 293, 231; (ESI) 523.1, 525.2, 293.0, 231.1.

Synthesis of [Cu(QnED)$_2$]PF$_6$ (20). Yield: 60.0%. ^{1}H NMR (DMSO-d_6): 6.55 (s, 4H), 7.68 (s, 4H), 7.84 (s, 4H), 8.03 (s, 4H), 8.17 (brs, 4H), 8.72 (brs, 4H), 9.07 (brs, 4H). ^{13}C NMR (DMSO-d_6): 91.57 (C_{quart}), 95.60 (C_{quart}), 117.30 (C_{quart}), 121.39 (CH), 128.16 (C_{quart}), 128.90 (CH), 129.28 (CH), 129.41(CH), 132.22 (CH), 140.45 (CH), 146.61 (C_{quart}), 152.89 (CH). IR (KBr, cm^{-1}): 3052, 2963, 2186, 1568, 1495, 1401, 1333, 1045, 913, 837, 779, 750, 557. MS (FAB): 723, 725 (M^+ calcd for $C_{48}H_{28}N_4Cu$: 723, 725), 393, 331; (ESI) 723.1, 725.0, 393.0, 331.1.

Results and Discussion

Syntheses. The 3-ethynylpyridine and 3-ethynylquinoline starting materials used in the preparation of metal-binding enediyne ligands were prepared by a modified literature method.[52] In general, reaction of 3-bromopyridine (**1**) or 3-bromoquinoline (**2**) with 1.2 equiv of trimethylsilylacetylene in diisopropylamine at 80−85 °C afforded the desired products (**3**, **4**) in excellent yield (85−90%). Hydrolysis of **3** and **4** in K_2CO_3/MeOH led to the formation of 3-ethynylpyridine (**5**) or 3-ethynylquinoline (**6**), respectively, in 55−65% yield (Scheme 1).

The enediyne ligand 1,6-bis(pyridine-3)hex-3-ene-1,5-diyne (**7**) was prepared by the addition of 2.2 equiv of **5** to *cis*-1,2-dichloroethylene over a Pd(0) catalyst, in the presence of CuI and *n*-BuNH$_2$ in benzene at 40−45 °C (Scheme 2). At 25 °C, this reaction is very slow and the yield of the desired product is poor. However, at 40−45 °C, the reaction proceeds rapidly to completion within 1 h. The crude product was isolated by solvent evaporation and purified by flash chromatography. Enediyne ligands **8**−**10** were prepared by a similar approach and characterized by ^{1}H and ^{13}C NMR as well as mass spectrometry.

The Cu(II) complexes **11**−**14** of enediyne ligands **7**−**10** were synthesized by reacting a 2:1 molar ratio of a designated ligand with $Cu(NO_3)_2 \cdot 2.5H_2O$ in MeOH at ambient temperature. The analogous CuN_2Cl_2 compounds **15**−**18** were prepared by reacting enediyne ligands **7**−**10** with $CuCl_2 \cdot 2H_2O$ in a 1:1 stoichiometry in MeOH, followed by repeated MeOH washings (Scheme 3). The corresponding Cu(I) complexes **19** and **20** were obtained by reaction of **7** and **8**, respectively, with $[Cu(CH_3CN)_4]PF_6$ in a 2:1 molar ratio in degassed MeOH under a nitrogen atmosphere (Scheme 4). The identities of these copper metalloenediynes were confirmed by ^{1}H,^{13}C DEPT NMR (for Cu(I) complexes), elemental analyses, and mass spectrometry.

X-ray Structure of 8. An ORTEP illustration of the X-ray crystal structure of **8** cocrystallized with one molecule of acetonitrile is shown in Figure 1. Crystal data and refinement parameters are given in Table 1, with selected bond lengths and angles listed in Table 2. The structure further confirms the identity of enediyne ligand **8** and illustrates that the molecule is in the cis conformation prior to metal coordination. The alkyne carbons are nearly linear with C1—C10—C11 and C10—C11—C12 bond angles of 174.2° and 177.9°, respectively. Although the enediyne linkage of the structure is essentially planar (deviation: 0.0025 Å), the quinoline rings are symmetrically rotated away from each other by 26° relative to this plane in order to minimize steric interactions of the hydrogen atoms. The separation of the alkyne termini is 4.29 Å, which is in the range expected for thermally stable acyclic enediynes.

Thermal Reactivity. The solid state thermal reactivities of enediynes **7**−**20** were measured by DSC and are arranged in Table 3 by enediyne ligand and their corresponding copper complexes. Each enediyne in Table 3 is a solid material at ambient temperature; however, the melting points for the enediyne ligands lie below their Bergman cyclization temperatures. Thus, the cyclization temperatures of the ligands are effectively recorded on samples in the neat liquid phase. This is not the case for the copper complexes as their melting points are at or above their Bergman cyclization temperatures as melting transitions are not observed by DSC. Therefore, caution must be used when comparing DSC temperatures between organic and inorganic materials.[53]

Figure 2a illustrates the DSC traces for the thermal cyclization of the bis(pyridine) enediyne ligand **7** and its benzannulated

(52) Sakamoto, T.; Shiraiwa, M.; Kondo, Y.; Yamanaka, H. *Synthesis* **1983**, 312−314.

(53) The phase influence on the Bergman cyclization temperatures of amine-containing enediyne ligands may be evaluated by preparing the HCl salt of the compounds and comparing cyclization temperatures determined by DSC. Unfortunately, for the enediyne ligands reported herein, the corresponding HCl salts exhibited melting points below the Bergman cyclization temperatures. However, for 1,8-bis(diamino)-oct-4-ene-2,6-diyne, no melting point is observed and the cyclization temperature of the HCl salt shows an increase of 121 °C over the compound in the neat liquid phase. This trend is also observed in solution as uncomplexed ligands often exhibit reactivity at higher temperatures than their corresponding metal complexes.[49] The correlation is sensible as free ligands such as **8** have larger separations between alkyne termini (4.29 Å) than the resulting metal complexes yet in some cases exhibit lower cyclization temperatures (in the liquid phase) than their inorganic counterparts (see Table 3).

Scheme 2. Pd-Catalyzed Coupling of Substituted Alkynes with Appropriate Dihalides To Yield Enediyne Ligands **7**−**10**

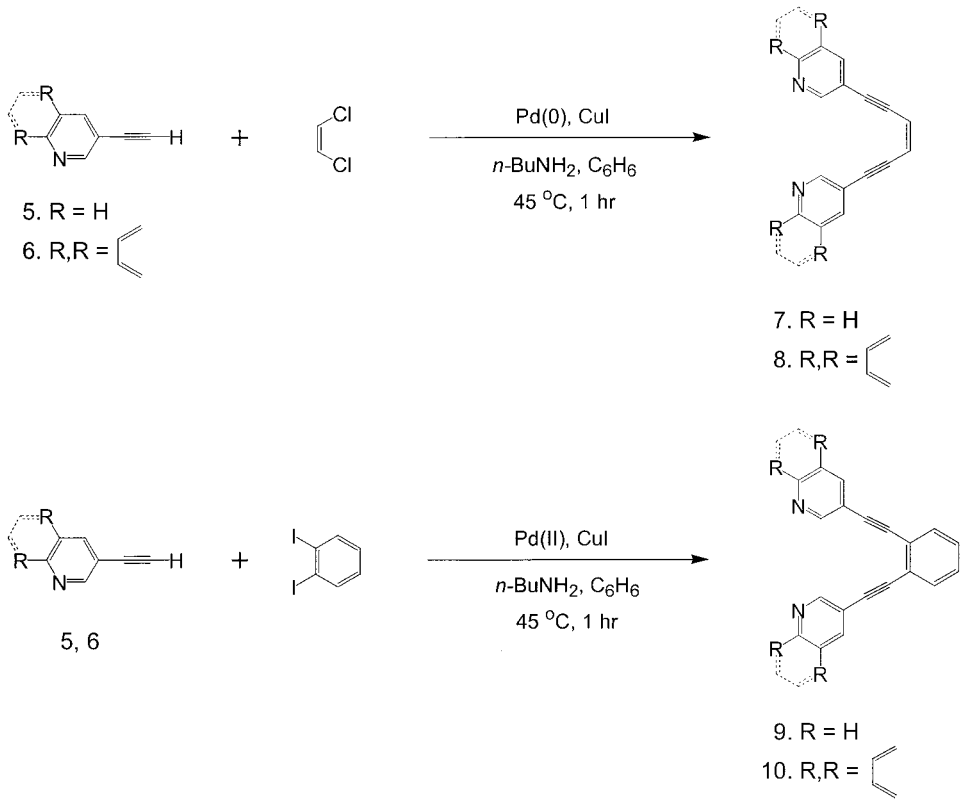

analogue **9**. These ligands exhibit broad exothermic peaks at 194 and 264 °C, respectively. Interestingly, their quinoline counterparts **8** and **10** possess cyclization temperatures (**8**, 195 °C; **10**, 272 °C) nearly identical to those of **7** and **9**, demonstrating that substitution of quinoline for pyridine at the alkyne termini does not significantly affect the thermal reactivities of these compounds. However, for a specific chromophore, substitution of benzene for diyl within the enediyne framework introduces significant stability to the ground state of the enediyne[16,54] as reflected in a ∼70−80 °C increase in the Bergman cyclization temperatures between chromophore analogues **7** and **9**, as well as **8** and **10**.

The copper complexes of **7**−**10** follow the same trends revealed in the cyclization temperatures for the free ligands. The Cu(II) bis(pyridine) (**11**) and bis(quinoline) (**12**) enediynes exhibit cyclization temperatures that are ∼50 °C lower than their benzannulated analogues **13** and **14**. More interestingly, the Bergman cyclization temperatures for the copper complexes of these ligands are intimately modulated by the oxidation state and nature of the ligands about the copper center. For the sequence **11**, **15**, **19**, the DSC profiles (Figure 2b) reveal exothermic peaks at 156, 256, and 326 °C, respectively, indicating stabilization of the enediyne unit proceeding from $[Cu(enediyne)_2]^{2+}$ to $Cu(enediyne)Cl_2$ and, finally, $[Cu(enediyne)_2]^{+}$. The same trends hold for the Cu(II) complexes of the benzannulated ligand **9**, the specific temperatures (**13**, 207 °C; **17**, 275 °C) of which derive from an increase in stabilization of the enediyne due to the additional delocalization of the π electrons. The Cu(II) complexes of the quinoline ligands **8** and **10** also obey this trend as identical temperature increases of 55 °C are observed on going from the bis(enediyne) (**12**, 171 °C; **14**, 230 °C) to the enediyne dichloride (**16**, 236 °C; **18**, 285 °C). Due to the high thermal cyclization temperatures of these Cu(II) analogues, and that of **19** (326 °C), the Cu(I) complexes of **8**−**10** were not synthesized as their DSC temperatures would likely exceed the limits of the DSC measurement.

The ability of the ligand to conformationally respond to metal complexation can be evaluated to a first approximation by determining the difference between the cyclization temperatures for the uncoordinated enediyne ligand and corresponding metal bound complex (Table 3). The response provides a relative measure of the influence that metal coordination has on the cyclization temperature of the enediyne unit. To calibrate the response, the phase of the enediyne sample at the cyclization temperature must be considered. The DSC temperatures of the enediyne ligands are essentially measured as neat liquids as their melting points lie below their Bergman cyclization temperatures, whereas for the metal complexes the opposite is true. Thus the magnitude of the decrease (+) or increase (−) in the cyclization temperature relative to the free ligand is not the only important parameter. Rather, the range in the cyclization temperatures for metal complexes of a given ligand in variable geometries is also significant for determination of ligand response to metal complexation. To this end, the responses of ligands **7**−**10** to copper complexation show pronounced variations in the cyclization temperatures, even for complexes with the same metal−ligand stoichiometries (Table 3). The most significant of these differences involve complexes **11** and **19** where the cyclization temperature of the enediyne unit is modulated by as much as 170 °C by simply changing the oxidation state of the copper center. This observation further demonstrates the utility of metal ions for controlling the Bergman cyclization temperature of a given enediyne chelate. Similar results are also observed between copper quinoline complexes **12** and **20** for which the cyclization temperatures vary by 114 °C. On the basis of previous work,[48,49] these trends derive from variations in the

(54) Semmelhack, M. F.; Neu, T.; Foubelo, F. *J. Org. Chem.* **1994**, *59*, 5038−5047.

Scheme 3. Complexation of Enediyne Ligands **7**−**10** To Yield $[Cu(N)_4]^{2+}$ or $Cu(N_2)Cl_2$ Structures

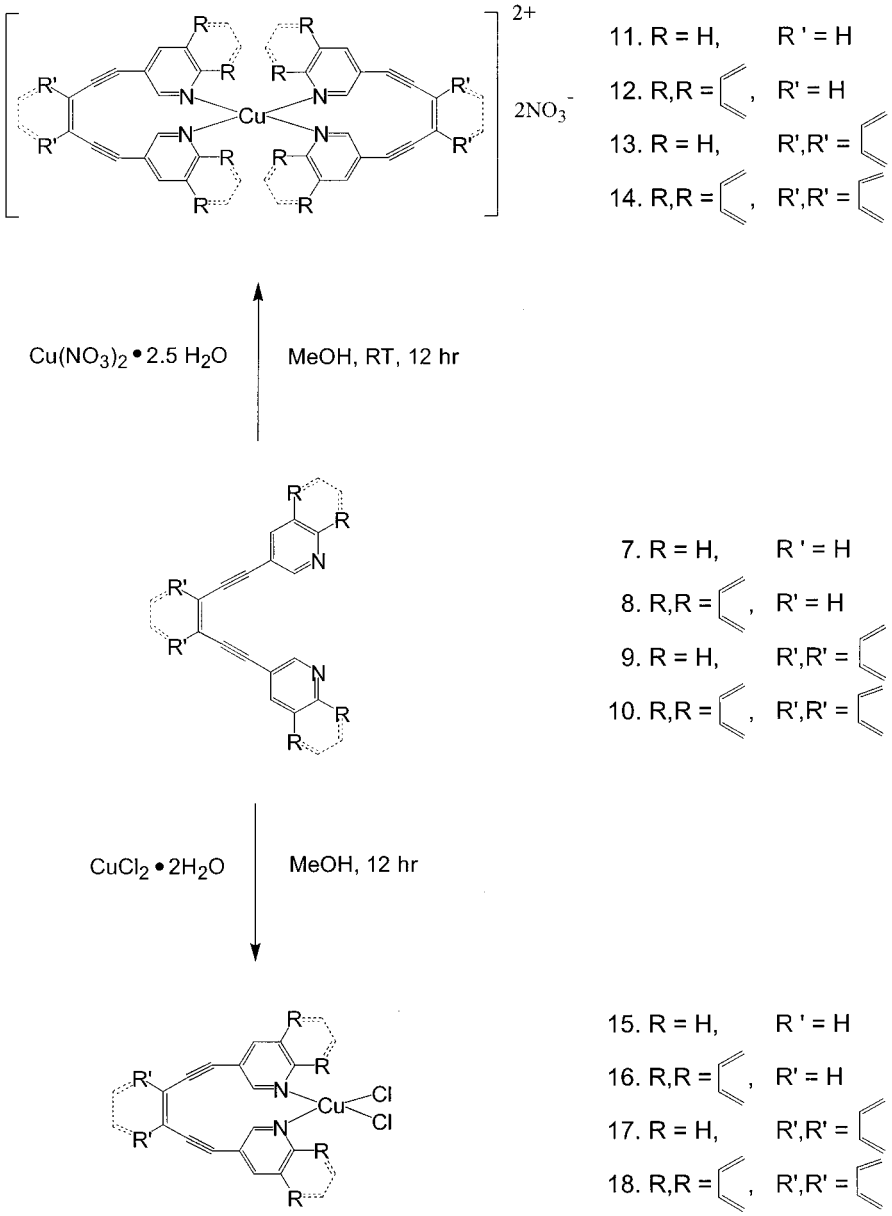

Scheme 4. Synthesis of Cu(I) Metalloenediynes **19**−**20** from Ligands **7** and **8**

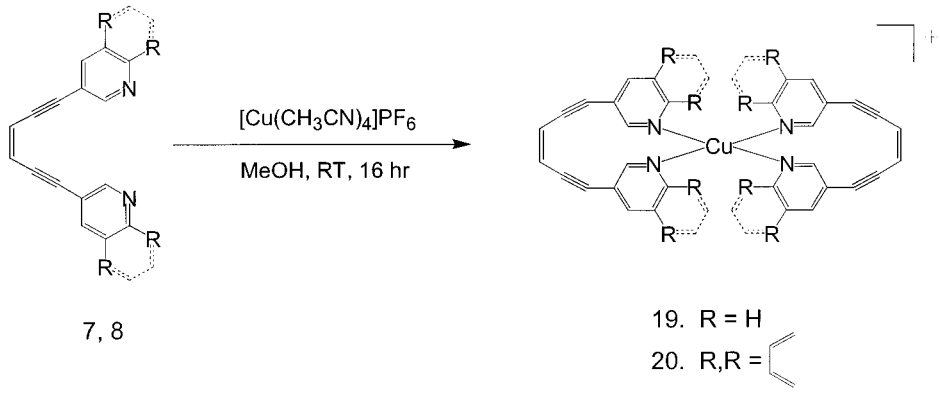

geometry of the copper center, which influences the conformation of the bound enediyne ligand and hence the thermal cyclization temperature of the complex (vide infra).

Electronic Spectroscopy of 11−**18.** The wealth of crystallographically characterized copper complexes with N_4 and N_2Cl_2 ligation, as well as their corresponding Cu(II) ligand field region electronic absorption spectra, permits evaluation of the local metal center geometry using UV−vis spectroscopy.[55] On the basis of the crystal structures of analogous tetrakispyridine complexes and simple ligand field theory arguments, the Cu(I)

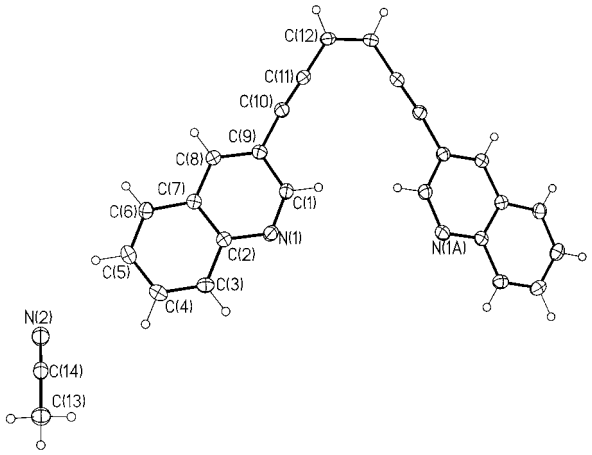

Figure 1. ORTEP diagram of the X-ray crystal structure of **8**. Thermal ellipsoids are illustrated at 30% probability.

Table 1. Crystallographic Data for **8**

formula	$C_{26}H_{17}N_3$
fw	371.43
cryst color habit	yellow rod
cryst syst	orthorhombic
space group	*Pnma*
a, Å	8.3605(7)
b, Å	18.2233(15)
c, Å	12.9522(10)
V, Å^3	1973.3(3)
Z, Z′	4, $^1/_2$
ρ_{calcd}, g/cm^3	1.25
T, K	173(2)
μ(Mo Kα), cm^{-1}	0.75
diffractometer	Siemens P4/CCD
radiation	Mo Kα (λ = 0.71073 Å)
$R(F)$, %[a]	3.85
$R(wF^2)$, %[a]	9.41

[a] Quantity minimized = $R(wF^2) = \sum[w(F_o^2 - F_c^2)^2/\sum[(wF_o^2)^2]^{1/2}$; $R = \sum\Delta/\sum(F_o)$, $\Delta = |(F_o - F_c)|$; $w = 1/[\sigma^2(F_o^2) + (aP)^2 + bP]$, $P = [2F_c^2 + \mathrm{Max}(F_o,0)]/3$.

Table 2. Selected Bond Distances (Å) and Angles (deg) for **8**

C(9)−C(10)	1.4267(17)	C(12)−C(12)#1	1.344(2)
C(10)−C(11)	1.1980(17)	C(23)−C(24)	1.175(9)
C(11)−C(12)	1.4126(17)		
C(8)−C(9)−C(10)	123.96(11)	C(10)−C(11)−C(12)	179.01(14)
C(1)−C(9)−C(10)	118.72(11)	C(12)#1−C(12)−C(11)	123.97(7)
C(11)−C(10)−C(9)	174.50(13)		

complexes **19** and **20** would be expected to possess tetrahedral geometry with a dihedral angle near 90°.[56−59] In contrast, Cu(II) complexes with N_4 and N_2Cl_2 ligand fields can adopt coordination numbers from 4 to 6[60] and have geometries ranging from square planar[61,62] to cis[63,64] or trans[65−70] distorted-octahedral. Typically, 4-coordinate square planar complexes exhibit three optical absorption features ($^2B_{1g} \rightarrow {}^2A_{1g}$, $^2B_{1g} \rightarrow {}^2B_{2g}$, $^2B_{1g} \rightarrow {}^2E_g$ in D_{4h}) between 17 000 and 20 000 cm^{-1} corresponding to transitions from d_{z^2}, d_{xy}, and $d_{xz,yz}$ to $d_{x^2-y^2}$ orbitals, respectively. For 6-coordinate tetragonal structures, this envelope is shifted to lower energy (11 000 to 17 000 cm^{-1}) as the ligand field splitting of the d orbitals is reduced due to the acquisition of an octahedral structure. Both of these geometries are readily distinguished from pseudotetrahedral structures for a given ligand set as the latter typically exhibit d−d bands between 5000 and 14 000 cm^{-1} depending upon the strength of the specific ligand field and the degree of compression of the tetrahedron toward the square plane. For a specific ligand set, the greater the distortion toward square planar, the higher the transition energies and vice versa.[55,71]

Table 3. Bergman Cyclization Temperatures for **7**−**20** Determined by DSC

compd (by class)	cyclization temp (DSC) (°C)	response rel to uncomplexed ligand (°C)
PyED (**7**)	194	
$[Cu(PyED)_2](NO_3)_2$ (**11**)	156	−38
$Cu(PyED)Cl_2$ (**15**)	265	+71
$[Cu(PyED)_2]PF_6$ (**19**)	326	+132
PybED (**9**)	264	
$[Cu(PybED)_2](NO_3)_2$ (**13**)	207	−57
$Cu(PybED)Cl_2$ (**17**)	275	+11
QnED (**8**)	195	
$[Cu(QnED)_2](NO_3)_2$ (**12**)	171	−24
$Cu(QnED)Cl_2$ (**16**)	236	+41
$[Cu(QnED)_2]PF_6$ (**20**)	290	+90
QnbED (**10**)	272	
$[Cu(QnbED)_2](NO_3)_2$ (**14**)	230	−40
$Cu(QnbED)Cl_2$ (**18**)	285	+13

We have used ligand field region electronic absorption spectroscopy to characterize the Cu(II) centers in these metalloenediyne complexes in the solid state (Table 4) in order to correlate the geometries of the metal centers with the observed Bergman cyclization temperatures. The electronic absorption profile for **11** (Figure 3a) exhibits a maximum (E_{max}) at 16 284 cm^{-1} which can be deconvoluted using three Gaussian band shapes centered at 17 626, 16 009, and 14 351 cm^{-1}. The energy of the individual transitions and overall absorption profile for a system with N_4 ligation indicate that the structure is 6-coordinate with little distortion from an octahedral ligand field.[72,73] Indeed, the structural assignment is corroborated by mass spectrometry and elemental analysis which show that the compound as prepared is a 6-coordinate bis(enediyne) species with two coordinated nitrate counterions. However, based solely on the

(55) Lever, A. B. P. *Inorganic Electronic Spectroscopy*, 2nd ed.; Elsevier: Amsterdam, 1984.
(56) Nilsson, K.; Oskarsson, A. *Acta Chem. Scand., Ser. A.* **1982**, *36*, 605−610.
(57) Dyason, J. C.; Engelhardt, L. M.; Healy, P. C.; Pakawatchai, C.; White, A. H. *Inorg. Chem.* **1985**, *24*, 1950−1957.
(58) Mak, T. C. W.; Goher, M. A. S.; Hafez, A. K. *Inorg. Chim. Acta* **1988**, *146*, 103−110.
(59) Wei, N.; Murthy, N. N.; Chen, Q.; Zubieta, J.; Karlin, K. D. *Inorg. Chem.* **1994**, *33*, 1953−1965.
(60) Addison, A. W.; Carpenter, M.; Lau, L. K.-M.; Wicholas, M. *Inorg. Chem.* **1978**, *17*, 1545−1552.
(61) Chan, C.-W.; Mingos, D. M. P.; White, A. J. P.; Williams, D. J. *Polyhedron* **1996**, *15*, 1753−1767.
(62) Koning, C. E.; Challa, G.; Hulstergen, F. B.; Reedijk, J. *J. Mol. Catal.* **1986**, *34*, 355.
(63) Fitzgerald, W.; Murphy, B.; Tyagi, S.; Walsh, B.; Walsh, A.; Hathaway, B. *J. Chem. Soc., Dalton Trans.* **1981**, 2271−2279.
(64) Fereday, R. J.; Hodgson, P.; Tyagi, S.; Hathaway, B. J. *J. Chem. Soc., Dalton Trans.* **1981**, 2070−2077.
(65) Haynes, J. S.; Rettig, S. J.; Sams, J. R.; Trotter, J.; Thompson, R. C. *Inorg. Chem.* **1988**, *27*, 1237−1241.
(66) Beurskens, G.; Martens, C. F.; Nolte, R. J. M.; Beurskens, P. T.; Smits, J. M. M. *J. Chem. Crystallogr.* **1995**, *25*, 425−427.
(67) Agnus, Y.; Labarelle, M.; Louis, R.; Metz, B. *Acta Crystallogr., Sect. C: Cryst. Struct. Commun.* **1994**, *50*, 536−538.
(68) Zhang, W.; Jeitler, J. R.; Turnbull, M. M.; Landee, C. P.; Wei, M.; Willett, R. D. *Inorg. Chim. Acta* **1997**, *256*, 183−198.
(69) Holzbock, J.; Sawodny, W.; Walz, L. *Z. Kristallogr.* **1997**, *212*, 115−120.
(70) Durand, P. B.; Holt, E. M. *Acta Crystallogr., Sect. C: Cryst. Struct. Commun.* **1995**, *51*, 850−852.
(71) Solomon, E. I. *Comments Inorg. Chem.* **1984**, *3*, 225−320.
(72) Batra, G.; Mathur, P. *Inorg. Chem.* **1992**, *31*, 1575−1580.
(73) Pradilla, S. J.; Chen, H. W.; Koknat, F. W.; Fackler, J. P. *Inorg. Chem.* **1979**, *18*, 3519−3522.

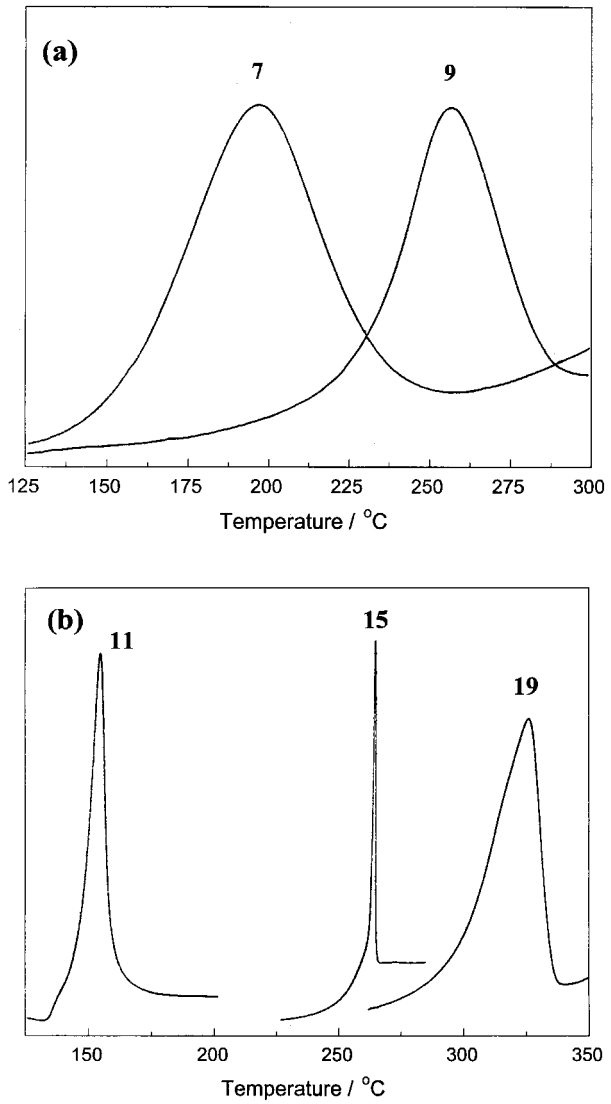

Figure 2. Differential scanning calorimetry traces for the thermal cyclization of (a) enediyne ligands **7** and **9** and (b) copper complexes **11**, **15**, and **19**.

Table 4. Solid State Electronic Absorption Band Energies for Enediyne Complexes of Cu(II)

compd	ligand field band energies/cm^{-1}			E_{max}/cm^{-1}
$[Cu(PyED)_2](NO_3)_2$ (**11**)	17 626	16 009	14 351	16 284
$Cu(PyED)Cl_2$ (**15**)	16 943	14 706	12 501	14 519
$[Cu(PybED)_2](NO_3)_2$ (**13**)	17 577	15 974	14 319	15 833
$Cu(PybED)Cl_2$ (**17**)	16 481	14 580	12 743	14 283
$[Cu(QnED)_2](NO_3)_2$ (**12**)	17 494	15 399	13 547	15 638[a]
$Cu(QnED)Cl_2$ (**16**)	17 280	15 110	13 292	14 833
$[Cu(QnbED)_2](NO_3)_2$ (**14**)	18 004	15 977	13 963	15 394
$Cu(QnbED)Cl_2$ (**18**)	15 719	13 964	12 238	14 051

[a] The value represents the center of the absorption profile determined at fwhm as the primary ligand field bands are experimentally resolved.

electronic absorption features, it is impossible to distinguish whether nitrogen or oxygen defines the Jahn−Teller axis.

In contrast, the d−d transitions (16 943, 14 706, 12 501 cm^{-1}) that comprise the absorption profile (E_{max} = 14 519 cm^{-1}) for the dichloride analogue **15** (Figure 3b) are red-shifted relative to **11** by 1300−1800 cm^{-1}. This can be accounted for by two distinct structural differences between the divalent copper dichlorides and their bis(enediyne) counterparts. First, mass

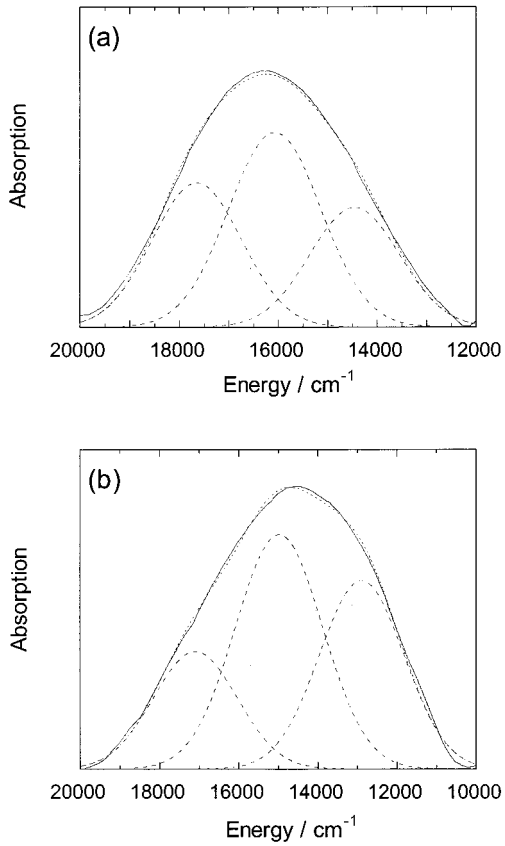

Figure 3. Ligand field region electronic absorption spectra of **11** and **15** in the solid state (Nujol) at 298 K. (a) The experimental spectrum for **11** (—) with E_{max} = 16 284 cm^{-1} can be fit by three Gaussian band shapes (- - -) centered at 17 626, 16 009, and 14 351 cm^{-1} and is plotted against the resultant sum (···) of these components. (b) The experimental spectrum for **15** (—) with E_{max} = 14 519 cm^{-1} is also deconvoluted with Gaussian band shapes (- - -) centered at 16 943, 14 706, and 12 501 cm^{-1} and is plotted against the sum (···) of these features.

spectrometry and elemental analysis indicate that **15** is a neutral, 4-coordinate compound in the solid state. Reduction in coordination number from 6 to 4 in a tetragonal Cu(II) system generally increases the ligand field splitting of the d-manifold and consequently the energy of the ligand field transitions. However, pseudo-σ and π donation to the copper center from the p orbitals of the chlorides reduces the ligand field splitting of the metal d manifold.[71] Second, the limited steric bulk of the chlorides, coupled with charge donation to the Cu(II) center, results in *cis*-CuN_2Cl_2 complexes that typically exhibit considerable dihedral angle distortions. Moreover, four of five structures in this class exhibit weakly distorted-to-tetrahedral geometries with angles ranging from $10° \leq \theta \leq 70°$.[74] These effects cause a reduction in λ_{max} for the electronic absorption profile[55] relative to 4-coordinate square planar and trans[75,76] Cu(II) complexes. Typically, 4-coordinate *cis*-CuN_2Cl_2 structures with pseudotetrahedral geometries exhibit absorption maxima between 11 000−14 000 cm^{-1}.[77] Since these transitions are somewhat lower in energy than those observed for **15** in the solid state, the structure

(74) The statistics for CuN_2Cl_2 structures were obtained from examination of 46 cis and 28 trans entries in the Cambridge Structure Database which could be associated with the desired structural class.
(75) McDonald, R. G.; Hitchman, M. A. *Inorg. Chem.* **1990**, *29*, 3074−3080.
(76) McDonald, R. G.; Hitchman, M. A. *Inorg. Chem.* **1990**, *29*, 3081−3088.
(77) Kokoszka, G. F.; Reimann, C. W.; H. C. Allen, J. *J. Phys. Chem.* **1967**, *71*, 121−126.

Table 5. Solid State EPR Parameters for Cu(II) Complexes of Enediyne Ligands **7**−**10**

compd	$g_{\|\|}$	$g_{\perp}$
$[Cu(PyED)_2](NO_3)_2$ (**11**)	2.15	2.07
$Cu(PyED)Cl_2$ (**15**)	2.19	2.10
$[Cu(PybED)_2](NO_3)_2$ (**13**)	2.15	2.07
$Cu(PybED)Cl_2$ (**17**)	2.20	2.08
$[Cu(QnED)_2](NO_3)_2$ (**12**)	2.27	2.07
$Cu(QnED)Cl_2$ (**16**)	2.16	2.07
$[Cu(QnbED)_2](NO_3)_2$ (**14**)	2.28	2.06
$Cu(QnbED)Cl_2$ (**18**)[a]	2.12	2.12

[a] A broadened isotropic signal is obtained due to paramagnetic Cu(II) interactions in the solid state yielding $g_{av} = 2.12$.

for **15** is best described as a cis 4-coordinate, flattened tetrahedron where the dihedral angle lies between planar and tetrahedral geometries (25−70°). The solid state structure proposed for **15** from the spectroscopic data is sensible since >75% of the *cis*-CuN_2Cl_2 structures in the Cambridge Structure Database exhibit degrees of dihedral distortion in this range.[74] The intermediate degree of distortion is also consistent with the solid state Bergman cyclization temperature for **15** which is between those of tetrahedral Cu(I) (**19**) and tetragonal Cu(II) (**11**) geometries.

The same trends are observed in the electronic spectroscopy of the benzannulated Cu(II) bis(pyridine) enediynes **13** (17 577, 15 974, 14 319 cm^{-1}; $E_{max} = 15\,833\ cm^{-1}$) and **17** (16 481, 14 580, 12 743 cm^{-1}; $E_{max} = 14\,283\ cm^{-1}$), which are distinguished by a 1550 cm^{-1} red shift for the dichloride analogue. The E_{max} values also compare very favorably with literature values, and with those of **11** and **15**, indicating that these compounds have comparable solid state structures. The tetragonal and pseudotetrahedral structures of **13** and **17**, respectively, are reflected in their Bergman cyclization temperatures as the distorted dichloride analogue exhibits a 68 °C increase relative to the tetragonal structure of **13**.

Comparison of the electronic absorption features for quinoline derivatives **12** and **16**, as well as benzannulated forms **14** and **18** (Table 4), reveals the same general trends in the component transitions and E_{max} values, indicating that although some variation in bond distances and dihedral angles may exist due to the increased steric bulk of the enediyne ligand, the compounds are generally similar in ligation and structure. Indeed, mass spectrometry and elemental analysis confirm bis(nitrato) hexacoordination for **12** and **14**,[78−80] while **16** and **18** are 4-coordinate, tetrahedrally distorted dichloro compounds.[81] The metal geometry-induced increase in the thermal cyclization temperature for the dichloride analogues is also conserved for the quinoline derivatives.

EPR Spectroscopy. In order to gain insight into metalloenediyne structure in the solid state, EPR signatures of the Cu(II) complexes **11**−**18** were obtained at 77 K (Table 5).[82] The spectra of the bis(enediyne) compound **11** (Figure 4a) reveals that the Cu(II) center is indeed axial ($g_{||} > g_{\perp} > 2.0$), with a $d_{x^2-y^2}$ ground state (in D_{4h}) and spin Hamiltonian parameters

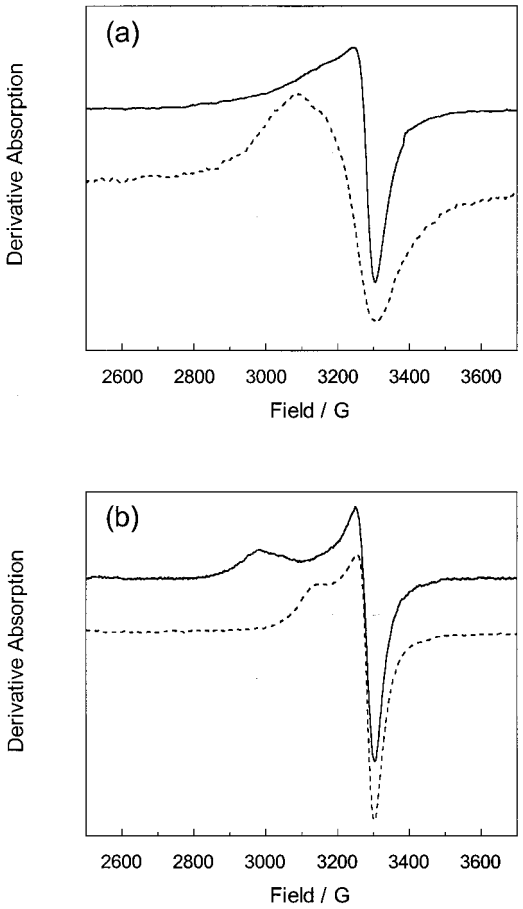

Figure 4. Solid state X-band EPR spectra of Cu(II) bis(enediynes) and their dichloride analogues at 77 K: (a) **11** (—), **15** (- - -); (b) **12** (—), **16** (- - -).

$g_{||} = 2.15$, $g_{\perp} = 2.07$. These values are typical for tetragonally elongated Cu(II) centers[83] and most closely correlate with tetragonal CuN_4O_2 structures ($g_{||} \sim 2.20$, $g_{\perp} \sim 2.00$).[73,84−86] The relatively low $g_{||}$ value suggests that the N_4 coordination comprises the primary ligand field with O_2 coordination from nitrate (vide supra), lying along the Jahn−Teller axis of the 6-coordinate structure.[83,87] Identical g values for the benzoenediyne analogue **13** indicate that the structural trend is not influenced by the presence of the aromatic ring on the enediyne backbone. The EPR spectral profile for the enediyne dichloride **15** appears markedly different from that for **13** (Figure 4a). However, spectral simulation demonstrates that the monoenediyne structure remains axial with both $g_{||}$ (2.19) and $g_{\perp}$ (2.10) shifted to lower field, consistent with chloride coordinated to the Cu(II) center. The g values correlate well with dihedrally distorted, 4-coordinate Cu(II) species containing *cis*-dichloride coordination.[77,87,88] Moreover, no half-field transition in the $g \sim 4$ region or significant deviations from $g \sim 2$ resulting from large zero field splitting are detected which rule out the existence

(78) Bukowska-Strzyzewska, M.; Skoweranda, J.; Heyduk, E.; Mrozinski, J. *Inorg. Chim. Acta* **1983**, *73*, 207−213.
(79) Moreland, J. A.; Deodens, R. J. *J. Am. Chem. Soc.* **1975**, *97*, 508−513.
(80) Kajikawa, Y.; Azuma, N.; Tajima, K. *Inorg. Chim. Acta* **1999**, *288*, 90−100.
(81) Savariault, J. M.; Galy, J.; Gutierrez-Zorilla, J. M.; Roman, P. *J. Mol. Struct.* **1988**, *176*, 313−322.
(82) Other methods for structure evaluation such as solution state EPR or X-ray crystallography were hindered by ligand dissociation in solvents displaying suitable compound solubilities.
(83) Peisach, J.; Blumberg, W. E. *Arch. Biochem. Biophys.* **1974**, *165*, 691−708.
(84) Davis, W. M.; Zask, A.; Nakanishi, K.; Lippard, S. J. *Inorg. Chem.* **1985**, *24*, 3737−3743.
(85) Comba, P.; Hambley, T. W.; Hitchman, M. A.; Stratemeier, H. *Inorg. Chem.* **1995**, *34*, 3903−3911.
(86) Uma, R.; Viswanathan, R.; Palaniandavar, M.; Lakshminarayanan, M. *J. Chem. Soc., Dalton Trans.* **1994**, 1219−1226.
(87) Hathaway, B. J. Copper. In *Comprehensive Coordination Chemistry*; Wilkinson, G., Ed.; Pergman: Oxford, 1987; Vol. 5, pp 533−774.
(88) Hathaway, B. J.; Billing, D. E. *Coord. Chem. Rev.* **1970**, *5*, 143−207.

of a strongly coupled $S = 1$ dimeric structure.[89] The same spectral profile is observed for the benzo analogue **17** which exhibits a more readily distinguisable $g_{||}$ feature at nearly the same value.

In contrast, EPR spectra of the quinoline derivatives indicates different trends in the solid state structures of the bis(enediyne) **12** and the monoenediyne dichloride **16** (Figure 4b). The spectrum of **12** reveals an axially elongated center with $g_{||} = 2.27$, which is considerably larger than that of the pyridyl analogue **11** ($g_{||} = 2.15$). Since both complexes exhibit axial spectra and have the same CuN_4O_2 coordination environments, the larger *g* anisotropy for the quinoline analogues must derive from differences in covalency resulting from variations in the identities of the weakly bound ligands along the Jahn−Teller axis in each system. Empirically, for Cu(II) $N_2O_2N_2'$ coordination, where N_2' designates weakly bound axial ligands, $g_{||}$ values are consistently larger than for their N_4O_2 counterparts indicating larger *g* anisotropy for systems with strongly bound oxygen ligands.[72,80,83] Since deviations in $g_{||}$ from the free electron value derive from spin−orbit coupling of the d_{xy} orbital into the $d_{x^2-y^2}$ ground state (in D_{4h}), the degree of metal−ligand covalency dictates the amount of orbital angular momentum localized on the copper center. The greater the covalent interaction, the smaller the *g* anisotropy.[87,88] This is consistent with the description of neutral, aromatic nitrogen ligands as strong field σ-donor/π-acceptors relative to weaker field, anionic nitrate oxygens (psuedo-σ/π-donors). When the latter are strongly bound in the *xy* plane, the result is enhanced d-orbital angular momentum localized on copper and hence larger $g_{||}$ values. This analysis suggests that the solid state structure of **12** is better characterized as Cu($N_2O_2N_2'$) with N′ being tetragonally elongated nitrogen from one of the quinoline functionalities.[80,83] This is consistent with our detection of free ligand **8** via hydrolysis of **12** in methanolic solutions over a 1 h period. Similar results are obtained for the benzannulated derivative **14**.

The spectral profile for the dichloride analogue **16** is once again axial, but unlike trends between **11** and **15**, the magnitude of $g_{||}$ is greatly reduced (2.16) while $g_{\perp}$ is virtually unchanged (2.07). The EPR parameters for **16** indicate a less distorted axial environment than observed for **15** or **17**, which suggests a decrease in the dihedral angle distortion, the magnitude of which is not readily accessible from these measurements. Interestingly, comparison of the Bergman cyclization temperatures for these compounds (Table 3) along the pyridine enediyne series **11** → **15** → **19** reveals that the cyclization temperature for **15** is considerably closer to that for **19** ($\Delta = 61$ °C) than that for **11** ($\Delta = 109$ °C), i.e., closer to tetrahedral in structure. In contrast, for the analogous quinoline series **12** → **16** → **20**, the cyclization temperature for **16** is closer to midway between those for **12** ($\Delta = 64$ °C) and **20** ($\Delta = 54$ °C), i.e., less tetrahedrally distorted. The electronic absorption data corroborate these minor differences in structure as the individual d−d transitions as well as E_{max} (**16**) are shifted slightly higher in energy than their corresponding values for **15**. Although more high resolution geometric and electronic structural information cannot be obtained from these spectra, the data indicate that these complexes are typical mononuclear Cu(II) structures with well-defined coordination spheres. Moreover, the combined optical and EPR data for these Cu(II) complexes correlate very well with crystallographically characterized N_2Cl_2[77,87,88] and N_4O_2[65−70] complexes.

Molecular Mechanics/Dynamics. Molecular mechanics calculations (MMX force field)[90] have been used effectively to correlate the thermal reactivities of metal-assisted Bergman cyclization reactions with the geometry of the enediyne and distance between alkyne termini.[45,48,49] We have developed a simulation protocol that involves calculation of plausible 4-, 5-, and 6-coordinate copper metalloenediyne structures using direct energy minimization, the starting points for which are determined on the basis of spectroscopic or crystallographically characterized models. Several of the lowest energy structures are then used as initial structures for molecular dynamics simulations to estimate the ground state structures under ambient conditions. In the dynamics simulations, the protocol allows the starting structures to access thermal bath modes at 800 K prior to cooling to a final sample temperature of 300 K. This approach yielded a structure for enediyne ligand **8** which exhibits a separation of alkyne termini (4.24 Å) and quinoline chromophore rotation angles (30.1°) that are comparable to those revealed in the X-ray structure of **8** shown in Figure 1.

To determine if structural consequences can account for the dramatic 170 °C variation in Bergman cyclization temperature across the series **11** → **15** → **19**, we have calculated the structures of these copper complexes using our molecular mechanics/dynamics protocol. As predicted by simple bonding theories, the 18-electron Cu(I) complex adopts a tetrahedral geometry of the CuN_4 core which is the dominant lowest energy structure and consistently reproduced from all initial geometric starting points (Figure 5). The average separation of alkyne termini, $\langle a \rangle$, was then calculated from the four tetrahedral structures lowest in energy. The relative energies of these structures range 5.6 kcal/mol with a modest standard deviation in the mean energy of 2.5%. From this structural subset, $\langle a \rangle$ was determined to be 4.20 Å for **19**, which correlates well with the high thermal requirements for Bergman cyclization of this complex and the coarse relationship between distance and cyclization temperature for synthetic enediynes.

The same dynamics approach was used in conjunction with the experimental data to assess the structure of the Cu(II) complex **11**. The geometry of **11** was initially modeled as a square plane of CuN_4 coordination with two OH ligands depicting axially bound nitrate counterions. The template structure was energy minimized producing a trans counterion geometry as the lowest energy structure. An ensemble of the four lowest energy tetragonal structures (range: 3.0 kcal/mol, SDEV = 1.2%) yielded an average distance between alkyne termini of $\langle a \rangle = 3.85$ Å.

For the dichloride analogue **15**, the cis conformation was the only minimized structure obtained. Interestingly, the structure is highly distorted toward tetrahedral geometry with an average dihedral angle of 70°, which yields $\langle a \rangle = 4.07$ Å (range: 3.5 kcal/mol, SDEV = 2.9%) from the four lowest energy structures. Within the 0.35 Å range in $\langle a \rangle$ between **11** and **19**, the $\langle a \rangle$ value for **15** falls 37% from that of the tetrahedral Cu(I) structure of **19**. A nearly identical deviation (36%) is observed in the Bergman cyclization temperature of **15** relative to **19**, indicating that the variation of distance with structure is at least partially responsible for the observed thermal reactivities of these copper metalloenediynes. Overall, these results show that the tetrahedral geometry of the Cu(I) centers causes significant distortion of

(89) (a) Hall, G. R.; Duggan, M.; Hendrickson, D. N. *Inorg. Chem.* **1975**, *14*, 1956−1964. (b) Kokoszka, G.; Duerst, R. *Coord. Chem. Rev.* **1970**, *5*, 209−244. (c) Ahmed, I. Y.; Abu-Hijleh, A. L. *Inorg. Chim. Acta* **1982**, *61*, 241−246.

(90) PCModel, Serena Software, Bloomington, IN 47405.

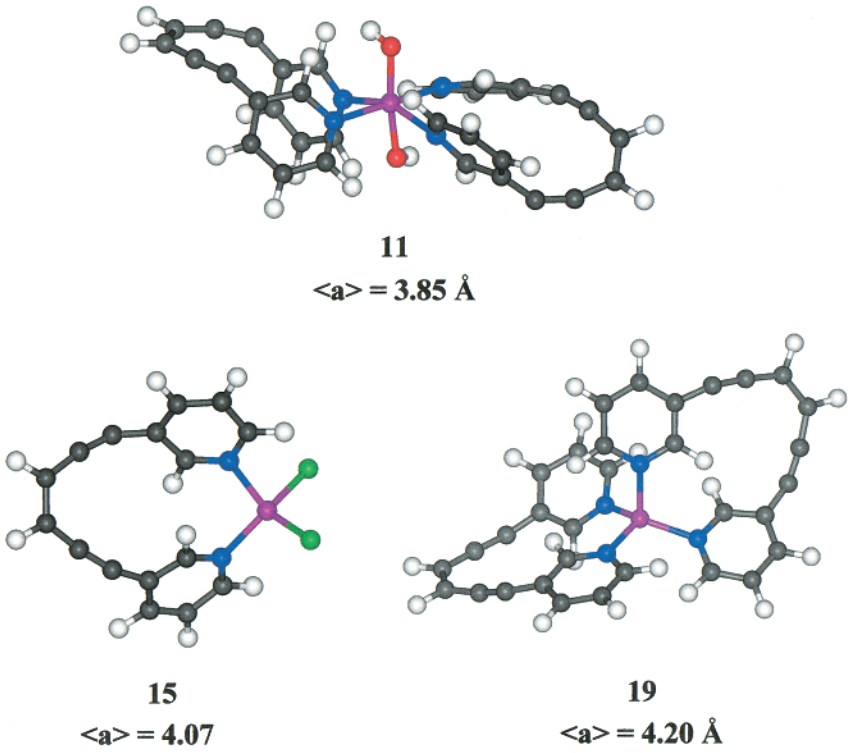

Figure 5. Geometric structures of copper metalloenediynes **11** ($\langle a \rangle = 3.85$ Å), **15** ($\langle a \rangle = 4.07$ Å), and **19** ($\langle a \rangle = 4.20$ Å) determined by molecular mechanics/dynamics calculations at the MMX force field level. Atom color designations: copper (pink), nitrogen (blue), oxygen (red), carbon (black), hydrogen (white), and chloride (green).

the enediyne unit and force the alkyne termini to a greater separation distance (0.35 Å) than the less strained tetragonal structures of the Cu(II) analogues. These results further document that the ground state electronic configuration of the metal can strongly influence the Bergman cyclization temperatures of bound enediyne ligands.[48,49]

Correlation of Metalloenediyne Reactivities. It has taken several years since the discovery of metal-assisted Bergman cyclization was first reported[45] to amass a subset of metalloenediyne complexes suitable for comparative evaluation of trends in thermal reactivities (Tables 3 and 6). The demonstration that the temperature at which 1,2-bis(diphenylphosphinoethynyl)-benzene (dppeb) cyclizes (243 °C) could be greatly reduced upon coordination to Pd(II) and Pt(II) while inhibited by Hg-(II) suggested that the reactivities of enediynes coordinated to various metals could be widely varied.[45] Subsequent demonstration that the tetrahedral geometry of a d^{10} Pd(0) center could strongly influence the cyclization temperature of dppeb[48] revealed that the ability of the ligand to respond to metal coordination geometry is an important factor in predicting metalloenediyne cyclization temperatures. This same trend has now been observed in the cyclization temperatures of the Cu(I) and Cu(II) complexes of 1,8-bis(pyridine-3-oxy)oct-4-ene-2,6-diyne (bpod),[49] as well as those reported in Table 3, illustrating that this is clearly one of the key parameters necessary for controlling metal-assisted Bergman cyclization reactions.

Unfortunately, an insufficient number of well-defined structural perturbations exist for a similar evaluation of other metal-binding enediyne ligands such as the bipydyl derivative of Konig et al. (dmbpyed),[47] as well as the tetraazaenediyne (taed) and bis(salicylaldimino) enediyne (bsded) macrocycles reported by Basak and co-workers[50,51] within this geometric paradigm. However, the Hg(II) complex of dmbpyed and the Cu(II) and Ni(II) complexes of taed each exhibit significant reduction in the Bergman cyclization temperatures relative to those of the free ligands, presumably due to analogous structural perturbations upon the enediyne framework.

Table 6. Comparison of Ligand and Metal Complex Cyclization Temperatures for Various Metalloenediynes

compd	cyclization temp (DSC)[a] (°C)	response rel to uncomplexed ligand (°C)	ref
dppeb	243	—	45
$Hg(dppeb)Cl_2$	>300	+ >57	45
$Pt(dppeb)Cl_2$	61	−182	45
$Pd(dppeb)Cl_2$	81	−162	45
$Pd(dppeb)_2$	222	−21	48a,b
$[Cu(dppeb)_2]PF_6$	227	−16	48b
$[Ag(dppeb)_2]PF_6$	266	+23	48b
bpod	136	—	49
$Cu(bpod)_2PF_6$	202	+66	49
$[Cu(bpod)_2](NO_3)_2$	121	−15	49
$[Cu(bpod)(py)_2]PF_6$	194	+58	49
$[Cu(bpod)(py)_2](NO_3)_2$	116	−20	49
$Cu(bpod)Cl_2$	152	+16	49
dmbpyed	237	—	47
$Hg(dmbpyed)(CH_3COO)_2$	145	−92	47
taed	~255[b]	—	50,51a
$[Ni(taed)](PF_6)_2$	~140[b]	~−115	51a
$[Cu(taed)](AcO)_2$	~110[c]	~−145	50,51a
bsded	179	—	51b
$[Ni(bsded)](ClO_4)_2$	276	+97	51b
$[Cu(bsded)](AcO)_2$	235	+56	51b

[a] Value obtained from the maximum of the reported DSC trace unless otherwise noted. [b] Temperature obtained by interpolation at reported DSC trace maximum. [c] The DSC trace for the Cu(II) complex was not provided in the reference. The value was estimated by using the reported onset temperature for the DSC peak (90 °C) and assuming the same fwhm of the trace reported for the Ni(II) analogue.

Beyond the structural perturbations to the enediyne conformation resulting from a given metal center geometry, the data in Tables 3 and 6 show that the size of the chelate and flexibility

of the enediyne ligand itself are also emerging as important contributors to the temperatures at which the resulting metal complexes undergo Bergman cyclization. Evaluation of the ligand response, however, is complicated by the fact that the ligand cyclization temperatures are typically recorded on samples with melting points below their reaction temperatures while the corresponding metal complexes cyclize in the solid phase as they do not exhibit melting points prior to reaction. Thus, there is an important phase difference between these measurements which does not permit the thermodynamics associated with these values to be compared straightforwardly, as reactivity in the solid state for a given compound may be expected to be greater than that in liquid form.[53] In the absence of these data, only relative deviations ($\pm$ °C) in the cyclization temperatures of the respective metal complexes from each other, or in cases where multiple complexes are not known, the free ligand values, can be used as a measure of the ligand response to metal complexation.

Comparisons of metalloenediyne structures with corresponding thermal reactivities (Tables 3 and 6) empirically suggests that the more rigid the enediyne ligand and the smaller the chelate size, the greater the response of the ligand to metal complexation. For example, the eight-membered chelate dppeb, which is the only enediyne to contain a metal-binding heteroatom adjacent to an alkyne carbon, exhibits the greatest response to metal complexation ($\Delta > 239$ °C between Pt(II) and Hg(II)). Large ligand responses are also observed for the rigid, 12-membered chelate PyED between Cu(II) and Cu(I) complexes **11** and **19**, respectively ($\Delta = 170$ °C). In contrast, the analogous Cu(I) and Cu(II) bis(enediyne) complexes of bpod, which is a 16-membered chelate containing additional oxygen and carbon atom spacers, exhibit a reduced range of response to metal complexation ($\Delta = 81$ °C) relative to **11** and **19**.[49] However, the flexibility afforded by the additional aliphatic atoms in the chelate dramatically reduces the thermal cyclization temperature of bpod itself relative to any of the other chelating enediyne ligands in Tables 3 and 6. Thus, ligand rigidity and range of ligand response are not necessarily the only features to be considered when designing metalloenediyne complexes for controlling Bergman cyclization reactions. Rather, increased flexibility of the enediyne can dramatically lower the thermal barrier to ligand cyclization, which is the starting point for metal perturbations on the cyclization thermodynamics. Increased flexibility and lower ligand cyclization temperatures do, however, come at the expense of ligand response to chelation and changes in metal geometry.[91]

Conclusion

These results further document the prominent role that metal complex geometry can play in the Bergman cyclization temperatures for bound enediyne ligands. The reactivities of the novel pyridine and quinoline enediynes and their corresponding copper metalloenediyne complexes described herein are in accordance with our previous reports of metal geometry dependent control of thermal Bergman cyclization temperatures. The structure/reactivity correlation more thoroughly accents the importance of the relationship between metal center geometry and Bergman cyclization reactivity. In addition, the increased cyclization temperature of these more rigid bis(pyridine) and bis(quinoline) enediyne ligands highlights a connection between enediyne flexibility, cyclization temperature, and response to metal complex geometry. The results show that more rigid chelates have higher free ligand Bergman cyclization temperatures, but enhanced responses to changes in metal complex geometry. This suggests that two approaches to designing controlled metalloenediyne reactivities are possible, namely, metal complexation by rigid ligands with large responses to metal coordination, and more subtle metal-mediated modulation of flexible enediyne ligands with already reduced thermal cyclization temperatures. Research into these areas in currently underway.

Acknowledgment. We thank Drs. Mark Pagel and Ulrike Werner-Zwanziger of the Indiana University NMR Facility for technical assistance. The generous support of the American Cancer Society (RPG-99-156-01-C), the donors of the Petroleum Research Fund (PRF 33340-G4), administered by the American Chemical Society, and Research Corporation (Research Innovation Award RI0102 for J.M.Z) are gratefully acknowledged.

Supporting Information Available: Crystallographic data for **8** including complete tables of bond distances and angles, final fractional coordinates, and thermal parameters. This material is available free of charge via the Internet at http://pubs.acs.org.

IC010014L

(91) The correlation is operable for the complexes discussed herein. However, caution must be applied when drawing comparisons across compounds with widely varying chemical compositions as functional group variations can strongly affect cyclization temperatures.